Improved Stereocontrol in Reductive Aminases through Steric Modification of Residues Around Substrate and Cofactor Binding Pockets

Jake Gooderham[1], Beatrice-Maria Zabava[1], David D. Aleku[1], Julie Vignot[1], Zuoye Xie[1], Ruth T. Bradshaw Allen[1], Mario Prejanò,[2]* Godwin A. Aleku[1]*

[1] Institute of Pharmaceutical Science, Franklin-Wilkins Building, King's College London, 150 Stamford Street, London SE1 9NH, United Kingdom.

[2] Department of Chemistry and Chemical Technologies, University of Calabria, Via Pietro Bucci 14/C, 87036 Arcavacata di Rende, CS, Italy.

* Correspondence: godwin.aleku@kcl.ac.uk; mario.prejano@unical.it

Section S1. Extended data

Table S1. Selected conserved bulky residues investigated in this work.

*Ma*RedAm	Conservation (from alignment of >400 homologues)
W33A	W (>99%)
R35A	R (99%) Q (<1%)
R104	R (86%) H (8.9%) W (1.2%)
Y118A	Y (99%), F(1%), W (0.2)
Y139	Y (96%) F (3.2%)
Y181	Y (98%) F (1.2%), W (0.2%)
W211A	W (92%) R (5.4%) F (2.2%) L (0.7%)

Table S2. Stereoselectivity of lysate and purified preparations of *Ma*RedAm WT, W35A and W211A variants across three different reductive amination reactions

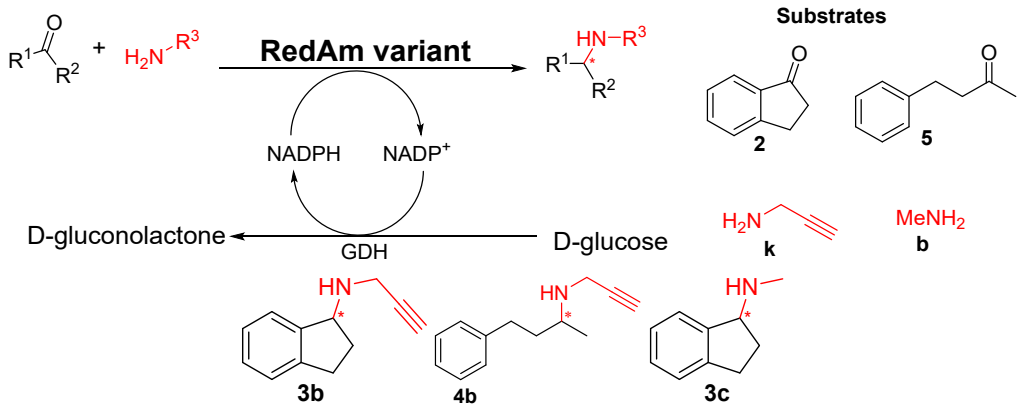

a. 48-h biotransformations characterised the stereoselectivity (*e.e.*) and conversion (%) %) using free lysate preparation of *Ma*RedAm variants (WT, *Ma*R35A and *Ma*W211A) across three different reductive amination reactions

Ketone	Amine	Product	Wild type		R35A		W211A	
			Mean Conv. (%) ± SD	Mean e.e. (%) ± SD	Mean Conv. (%) ± SD	Mean e.e. (%) ± SD	Mean Conv. (%) ± SD	Mean e.e. (%) ± SD
3	**b**	**3b**	46.7 ± 0.3	88.0 ± 1.4 (*R*)	36.4 ± 0.2	94.0 ± 0.9 (*R*)	44.2 ± 0.7	38.2 ± 1.2 (*S*)
3	**c**	**3c**	16.6 ± 0.6	44.4 ± 2.9 (*R*)	4.8 ± 1.0	65.7 ± 5.3 (*R*)	27.1 ± 0.5	93.5 ± 2.3 (*S*)
4	**b**	**3b**	>99.0 ± 0.1	63.0 ± 0.8 (*R*)	>99.0 ± 0.2	88.2 ± 1.0 (*R*)	>99.0 ± 0.2	51.8 ± 0.4 (*S*)

b. 24-h biotransformations analysed the stereoselectivity (*e.e.*) and conversion (%) of purified *Ma*RedAm variants (WT, *Ma*R35A and *Ma*W211A) across three different reductive amination reactions.

Ketone	Amine	Product	Wild type		R35A		W211A	
			Conv. (%)	e.e. (%)	Conv. (%)	e.e. (%)	Conv. (%)	e.e. (%)
3	**b**	**3b**	35.5	73.9 (*R*)	35.5	91.8 (*R*)	30.1	42.4 (*S*)
3	**c**	**3c**	22.7	6.3 (*R*)	14.7	35.8 (*R*)	15.6	95.8 (*S*)
4	**b**	**4b**	>99.0	29.3 (*R*)	>99.0	91.0 (*R*)	>99.0	70.4 (*S*)

c. 48-h biotransformations analysed the stereoselectivity (*e.e.*) and conversion (%) of purified *Ma*RedAm variants (WT, *Ma*R35A and *Ma*W211A) across three different reductive amination reactions.

Ketone	Amine	Product	Wild type		R35A		W211A	
			Conv. (%)	e.e. (%)	Conv. (%)	e.e. (%)	Conv. (%)	e.e. (%)
3	**b**	**3b**	48.2	59.5 (*R*)	53.1	91.9 (*R*)	43.0	40.4 (*S*)
3	**c**	**3c**	37.0	5.5 (*R*)	17.5	32.6 (*R*)	24.7	96.0 (*S*)

Table S3. Michaelis Menten constants of selected *Ao*IRED mutants.

(a) Michaelis Menten constants of *Ao*IRED N241X variants towards imine **2**

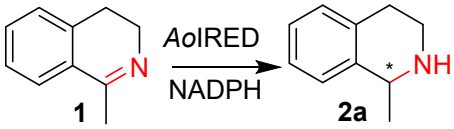

*Ao*IRED variants	K_m [mM]	k_{cat} [s^{-1}]	k_{cat}/K_m [$s^{-1}mM^{-1}$]
*Ao*IRED WT	0.718	0.743	1.034
N241H	0.261	0.506	1.934
N241A	0.349	0.719	2.054
N241S	0.351	1.661	4.730

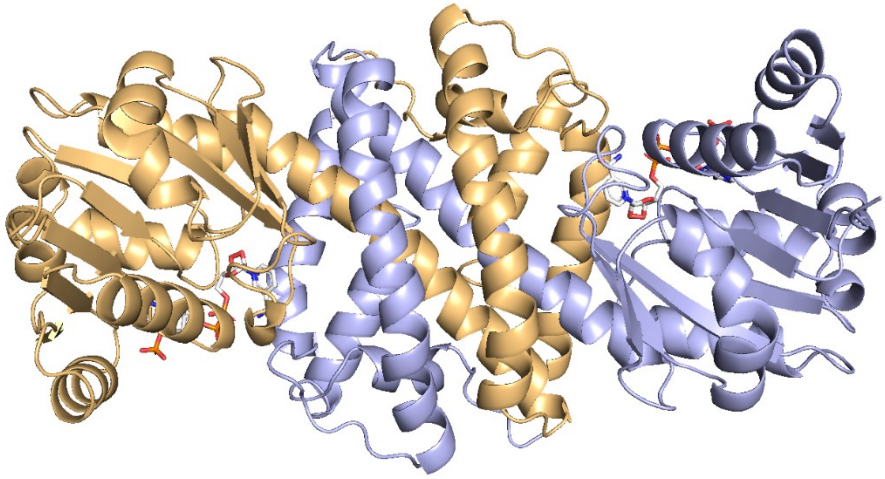

Figure S1. AlphaFold model of *Ma*RedAm dimer, with NADPH introduced to the model via Alphafill.

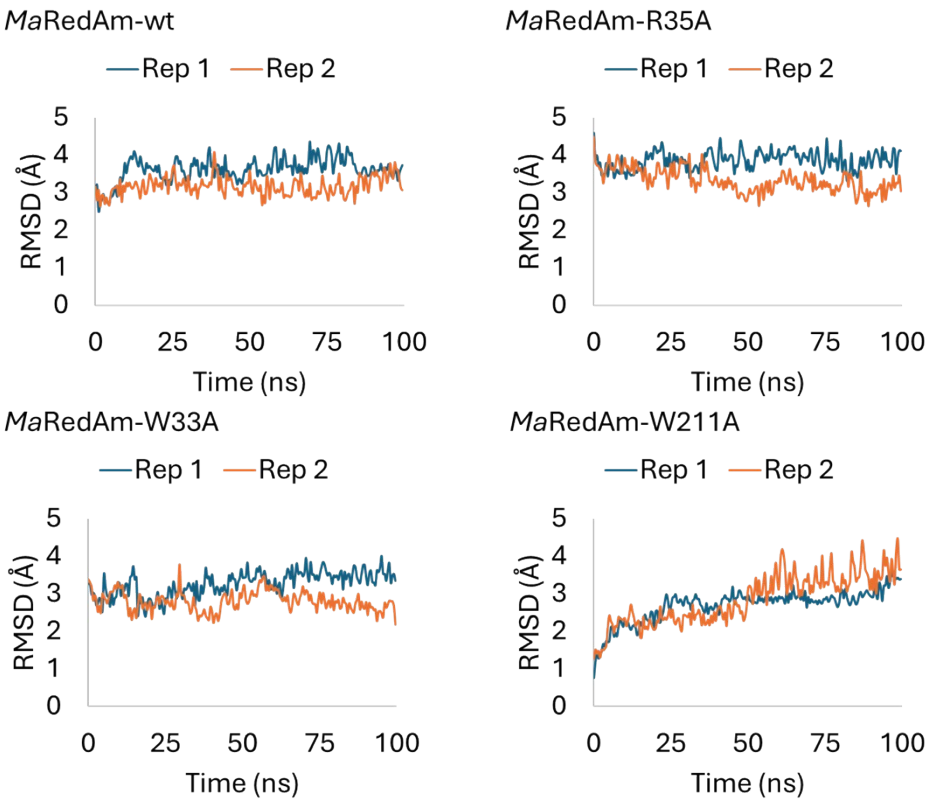

Figure S2. RMSD of protein backbone for each investigated system.

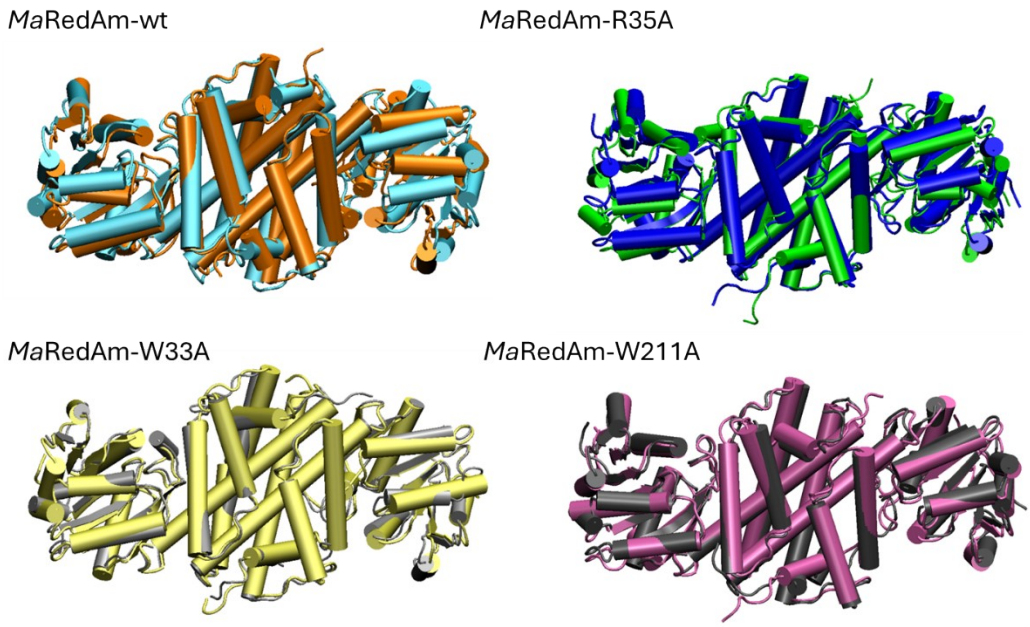

Figure S3. Overlays of most populated clustered structures obtained from replicas performed on each system.

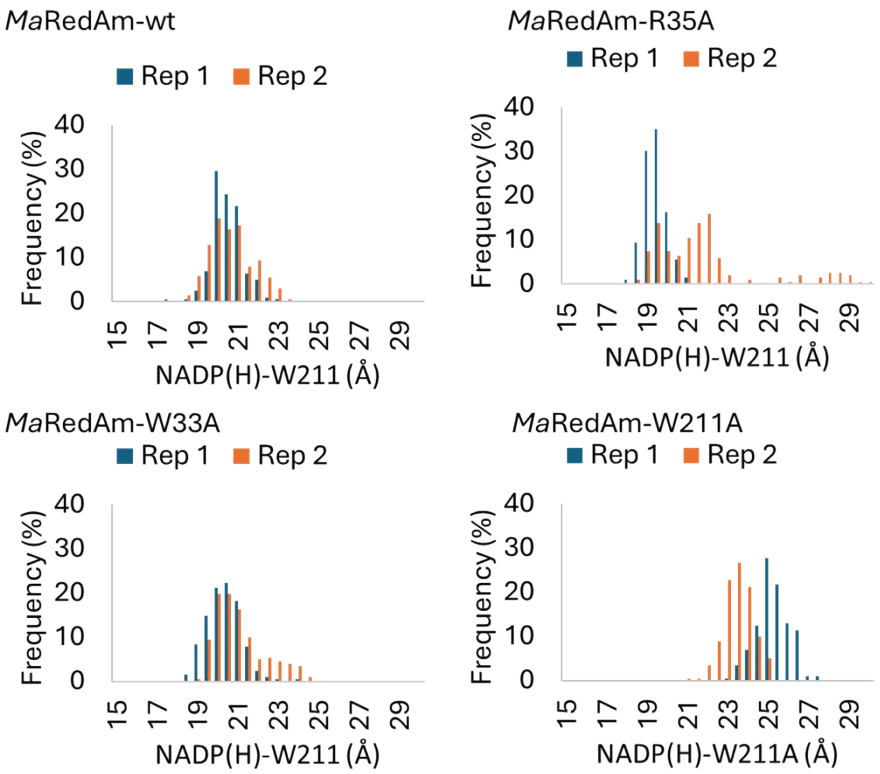

Figure S4. Frequencies distribution of NADP(H)-W211/W211A distances (centre of masses) observed during the simulations.

Section S2. Experimental Procedures

Chemicals and molecular biology reagents. Commercially available chemicals, inorganic salts, HPLC solvents, and reagents of high purity were purchased from Merck Life Science UK (Sigma-Aldrich, Dorset, UK), Fluorochem (Hadfield, UK), Thermo Fisher Scientific (Horsham, UK), and Acros Organics (Loughborough, UK). D-(+) glucose was also acquired from Merck Life Science UK (Sigma-Aldrich, Dorset, UK). Enzyme nicotinamide cofactors $NAD(P)^+$ and NAD(P)H were purchased from Cambridge Bioscience (Cambridge, UK). Media were purchased from Formedium (Hunstanton, UK).

The genes encoding IREDs/RedAms were codon-optimised for expression in *E. coli*, synthesised by Twist Biosciences (South San Francisco, USA), and cloned into a pET28a (+) vector. DNA primers were synthesised by Sigma-Aldrich (Dorset, UK). Chemically competent high-efficiency and subcloning efficiency *E. coli* cells (DH5α and BL21 DE3) were purchased from New England Biolabs (Hitchin, UK), as were the Q5 High-Fidelity PCR master mix, T4 Polynucleotide Kinase (PNK), T4 DNA ligase, and DpnI. FastDigest DpnI was obtained from Thermo Fisher Scientific (Horsham, UK). All gels, buffers, stains, and markers were also supplied from Thermo Fisher Scientific (Horsham, UK), as was the GeneJET plasmid miniprep kit for DNA and SDS-PAGE electrophoresis procedures. Lysozyme from chicken egg white, benzonase nuclease, and peroxidase from horseradish (P8250-5KU) were sourced from Merck Life Science UK (Sigma-Aldrich, Dorset, UK). In contrast, GDH 101 was sourced from Johnson Matthey (Cambridge, UK).

Primer design, mutagenesis, and library validation. The Protein sequence of *Ma*RedAm was used as a query sequence, and utilising protein BLAST, 1200 homologues were retrieved from non-redundant

protein databases available on NCBI. Using the UGENE bioinformatic tool, multiple sequence alignment was performed with MUSCLE to identify conserved bulky residues in the *Ma*RedAm homologue sequences. Bulky residues with high conservation scores (>90%) were selected for site-directed mutagenesis.

PCR Primers for mutagenesis were designed using NEbaseChanger and synthesised by Sigma-Aldrich. Site-directed mutagenesis was performed according to the NEB Q5® mutagenesis protocol using the wild-type RedAm plasmid as a template. 3 µL of PCR amplification products were analysed by agarose gel electrophoresis, while the remainder was stored at 4°C for ligation. Samples showing a band at ~ 6 kb (pET28a vector + RedAm insert) following agarose gel analysis were subjected to ligation. One-pot kinase-mediated phosphorylation, ligase-catalysed ligation, and DpnI-catalysed digestion (KLD reaction) were performed using a KLD (Kinase, Ligase, DpnI) cocktail prepared in-house. The KLD enzyme mix was prepared from 33.5 µL of T4 polynucleotide kinase (NEB M0201S), 2 µL of T4 DNA ligase (NEB M0202S), and 16.5 µL of DpnI (NEB R0176S), adapted from the recipe by DeMott et al.[1] The KLD buffer was prepared by adding 29 µL of ligase buffer with 71 µL of deionised water. 4 µL of PCR product, 2 µL of KLD enzyme mix, and 4 µL of KLD buffer were combined, and the resulting ligation mixture was incubated in an Eppendorf thermocycler at 24°C for 2 h, followed by 37°C for 1 h. The mixture was then used immediately for transformation or stored at 4 °C overnight.

Chemically competent *E. coli* DH5α cells were transformed with the KLD reaction product. Colonies were randomly picked from each plate, and plasmid preps (using GeneJET plasmid miniprep kit) isolated from 10-15 ml overnight cultures were sequenced (Sanger sequencing) and analysed to confirm that the target mutations had occurred.

Expression, Production, and Purification of Single-Point Mutants. Chemically competent *E. coli* BL21 (DE3) cells were transformed with a RedAm/IRED plasmid, plated on a kanamycin-containing agar plate, and incubated at 37 °C overnight. A single colony from this plate was used to innoculate LB broth (10 mL) containing kanamycin (final concentration 35 $\mu g mL^{-1}$) and cultivated overnight (37°C, 200 r.p.m), and this was used as the starter culture. A 2-L flask containing 500 mL of LB was supplemented with kanamycin (35 µg/mL).−1and inoculated with 5 ml of starter culture. Cultivation was performed at 37 °C in an orbital shaker with shaking at 180 r.p.m. At an optical density (OD600) of 0.6 to 0.8, isopropyl β-D-1-thiogalactopyranoside (IPTG, final concentration of 0.4 mM) induces protein expression. Incubation was continued at 22-25°C and 180 rpm for 18 hours. Cells were then harvested by centrifugation and washed in Tris-HCl buffer (100 mM, pH 7.5). For quick purification, cells were resuspended in buffer A (50 mM Tris-HCl, 300 mM NaCl, 25 mM imidazole, pH 7.5). Lysis reagents (1 mg mL-1 lysozyme from chicken egg white, 0.3 mg mL-1 polymyxin B, 1 µL mL-1 benzonase) were added to the resuspended cells and incubated at 20 °C for 2 h. Following centrifugation of the lysed cells (12,000 r.p.m, 4 °C, one h), the clarified lysate was purified by Ni-affinity chromatography using gravity columns. Clarified lysate was loaded onto the equilibrated column (prepacked with 5 mL of Ni-NTA agarose resin), followed by a single-step wash with buffer A, and then eluted with buffer B (50 mM Tris-HCl, 300 mM NaCl, 300 mM imidazole, pH 7.5). The elute was desalted using 10 kDa cut-off centricon filters (15 mL), and the buffer was exchanged for Tris-HCl buffer (50 mM Tris, 100 mM NaCl, pH 7.5)

Biotransformation. Biotransformation reactions were performed using cell-free extracts or purified enzyme preparations, employing glucose dehydrogenase (GDH)/$NADP^+$ as a cofactor recycling system. For the RedAm-catalysed reductive amination of ketones, a 500 µl reaction mixture contained 10 mM ketone, 100 mM amine partner, 30 mM D-glucose, 0.3 mg ml-1 GDH (lyophilised cell-free extract), and 0.5 mM NADP+ in Tris-HCl buffer (100 mM, pH 8.0) containing 2% (v/v) DMSO. Amine nucleophiles were supplied from a 1 M buffered amine nucleophile solution stock, pH 8. The reaction was initiated by the addition of 1 mg mL-1 purified RedAm or 200 µL of fresh lysate solution. The reaction volume was adjusted to 500 µl with Tris-HCl buffer (100 mM, pH 8.0). Reactions were incubated at 25 °C with shaking at 200 r.p.m. for 24 -48 h.

For analysis, reactions were quenched by adding 50 µL of 5 M NaOH and then extracted twice with 500 µL of tert-butyl methyl ether. The organic fractions were combined and dried over anhydrous MgSO4 and analysed on normal phase HPLC using chiral columns (CHIRALPAK®IC 250 mm × 4.6 mm, 5 µm; and CHIRALPAK® IB N-5, 250 mm × 4.6 mm, 5 µm). Samples were run at a flow rate of 1 mL/min and monitored at 265 nm.

AlphaFold model of *Ma*RedAm. *Ma*RedAm amino acid sequences were submitted to ColabFold.[2] (Alphafold2 using MMseqs2, v1.5.5) to generate monomeric PDB models. NADPH was introduced to both models via Alphafill,[3] With PDB 1TQN serving as the template for both models. The transplant clash score (RMSd of the Van der Waals overlap between ligand and polymer atoms) for MaRedAm and BacRedAm were 0.08 and 0optimised transplant clash scores for both models were 0.08 Å, indicating minimal steric interference. Dimeric structures were generated by aligning the monomeric models with PDB 5G6S in PyMOL (version 2.5.7). Enzyme-cofactor models were subsequently optimised using YASARA (version 18.4.24) energy minimisation to ensure stable interactions between the enzyme and cofactor.[4]

Molecular dynamics simulations. An AlphaFold model of *Ma*RedAm enzyme was selected as the starting structure to build up the model (**Figure S1)**. W33A, R35A and W211A mutations were added *via* tleap module as implemented in Amber20 package.[5] Geometry optimisation of NADP(H), **3** and **b** species was performed at HF/6-31G* level of theory to generate unbound charges and parameters, by fitting atomic charges *via* Merz–Singh–Kollman scheme with the RESP procedure[6] and GAFF,[7] respectively. The ligands (NADP(H), **3** and **b**) were placed in the model in analogy to *Asp*RedAm structure in complex with NADP(H) and amine product rasagiline (PDB= 5g6s),[8] and each 3D structure was later inserted in a TIP3P cubic water box (93x63x74 $Å^3$). After geometry-minimization, performed following a procedure adopted in previous studies,[9–11] the systems were gradually heated to 298 K for 10 ns, using the Langevin thermostat in the NVT ensemble. For the production, *Ma*RedAm-WT, *Ma*RedAm-W33A, *Ma*RedAm-R35A and *Ma*RedAm-W211A systems undergone to 2x100 ns of molecular dynamics (MD) simulations, for a total of 800 ns, at 298 K and 1 bar in NPT ensamble. MD simulations were carried out using Amber20 package, treating the protein with ff14SB force field,[12] using time constant τp=2.0 ps, the SHAKE algorithm, and Particle Mesh Ewald (PME) summation method, with an integration step of 2 fs and a cutoff radius of 10.0 Å.

In the preliminary step of the investigation, attention was focused on main structural parameters, such as RMSD and analysis of population *via* hierarchical clustering. From the analysis of the protein backbone, it can be noticed that the simulations have a reproducible trend, reaching the equilibrium in 100 ns, with RMSD values oscillating in 2-4 Å (see **Figure S2**). Such reproducibility can be further evinced by the superimposition of the most populated clustered structures obtained from MD simulations (see **Figure S3**). No relevant variations of secondary structures were observed, and thus, the analysis of the trajectories has been carried out in accordance with the results reported in the main manuscript.

Section S3. Gene sequences

>*Ma*RedAm
ATGACTTCTTCCTCCACTGTTAGCATTATCGGCCTTGGCGCCATGGGCTTGGCCCTTGCTGCCAAGTTTGTGGAG
AAGGGCTACACGACCACTGTTTGGAACAGATCCACCGAGAAGGCACTCAAGTTTGCTGCAGAGCACGAGAACGCG
CATGCCGCAACCACCGTGGCTCAAGGTCTAGAGGCTAGCAACCTGGTGATCATCTGTCTTCTCGACAACAAGGCC
GTTCGCGATACCATTGATCAAGCCCTTCCCTCCTTGGCGGGACGCATCGTTGTCAACCTGACTAACGGTACCCCT
GATGAGGGACGAGAGACTGGGGCCCTTGTGGCGGCTCAGGAAGGATCCAAGTACGTGCACGGCGGGATCATGGCA
ACTCCTTCGATGGTCGGCTCTCCGGCATCGGTGCTGCTGTACAGCGGATCTCTAGAAGCTTACACAGCGGTGGAG
AAGGATCTCGAGATCCTGGGTGCTGGCAAGTACCTCGGAGCCGACTCTGGATCGGCTTCGCTGCATGATCTGGCG
CTCCTGAGCGGGATGTATGGCCTCTTCTCTGGCTTTACGCATGCAGTGTCGCTGGTGCGGAACGAGAAGCGGTCG
ACCACGGAATTCCTGTCGCTTTTGGTGCCCTGGCTGACGGCGATGACGGGCTACCTGCACGTGCTGGGCAAGCAG
ATTGATGAGGGCGACTTCTCGTCTCTTGGGTCGAGTATTGAGATGCAGGTGCCTGCGATCAACAACATTGTGAAG
ACAAGCGAGGCACAGGGCGTGTCTGCGGATCTCATCCGGCCCATCCAAGGCTTGCTGGAGCGTGCGGTGGCGGTC
GGACGAGGTGGCGAGGAGATCTCGGCGCTGGTGGGCCTGAATGTGCTGGCGAGGAAGGCAGAGTAA

>*Am*IRED
ATGACAGATCAAAATCTACCCGTTACTGTAGCTGGCCTGGGTCCGATGGGTGCGGCGCTCGCTGCGGCGTTGCTG
GACAGAGGCCACGATGTTACCGTTTGGAACCGTAGCCCGGGCAAGGCTGCTCCGCTGGTGGCAAAAGGTGCGCGT
CAAGCGGACGACATCGTTGACGCGGTTAGCGCGAGCCGTCTGTTGGTGGTGTGCCTGGCGGATTACGATGCACTC
TACTCTGCCCTGGGCCCAGCGCGCGAGGCGTTGCGTGGTCGTGTGGTGGTAAATCTGAACAGCGGTACACCGAAA
GAGGCCCGTGAAGCAGCTCAGTGGGCAGAAGGTCACGGCATCGGTTACCTGGACGGCGCGATTATGGTTCCGCCA
CCTCTCGTCGGTCACACTGGTTCCTTGTTTCTGTACAGCGGTTCCACCGAGATCTTTGAAACCCATAAAGAAACT
CTGGCGGACCTGGGTGATCCGGCGCATCTGGGCACGGATCCGGGTCTGGCGGTGCTGTATAACACCGCATTGTTA
AGCATGATGTATTCTAGCCTGAACGGCTTCTTGCATGCGGCCGCTCTGGTGGGCTCTGCGGGTGTTGGTGCGGCA
GAGTTCACCGAGATTGCAGTCGACTGGTTCCTGCCGTCGGTCATCGGCGGTATCATCAAAGCCGAGGCTCCGACC
ATTGATAAGGGCGAATATCCGGGTGAACTGGCGAGTTTGGAAATGAATGTTACGACCTTGAAGCACATTATCGGC
ACCAGCGATGAACAGCGTGTTGACGCTGGCATTCCGGCAGGAAACAAAGAGCTGCTGGACCGCGCAGTGGCCGCG
GGCTTTGGTAAGAGCGGCTACTCCTCCGTGATTGAGGTTCTTAAGCGCGGTGCGGCTTAA

>*Ar*IRED
ATGAGTGAGAAGAAGCTGGCAGTTACCGTAGCAGGACTGGGGCCAATGGGTTCAGCCCTGGCCGCGGCACTGCTT
GATCACGGCCACGAAGTCACGGTATGGAATCGTAGTCCTGGTAAGGCTGCGCCGTTAGTAGCACGCGGTGCCCGC
GAAGCGGATGGCGTGGCTAGCGCAGTGAGCGCGTCTGAAGTAACTGTGGTGTGCCTTGCCGACTACAACGCGTTA
TACTCGGCGTTACGCCCAGCAGAGGCGGCTCTTCGTGGACGTGTGGTTGTGAATCTTAATAGCGGCACCCCCAAA
GAGGCACACGAAGCAGTCCGTTGGGCGGAAGACCGTGGTATCGGTTACTTGGACGGAGCTATTATGGTTCCACCC
GCGATGGTCGGACGCCCAGGCAGCGTATTCCTGTATTCTGGTGCAGAGGATGTATTTGATGCACACAAGGCGACC
CTGGCGGTTCTGGGTGAGGCAACGTACCTTGGTGCAGACCCAGGCCTTGCCGTACTTTACAATACGGCACTTCTG
TCTTTGATGTACAGCAGTATGAACGGCTTTCTGCACGCTGCGGCGCTGGTTGGCTCGGCGGGAGTTGCAGCGACG
GACTTCACAAAGCTGGCTGTTGACTGGTTCTTACCTAGTGTGGTCGGCGGCATTTTAGAAGTTGAGGCTCCAGCG
ATCGACAATGGTGTTTACCCTGGTGATTTAGGCTCATTAGAGATGAACTTAACGGCCTTGACCCATATTGTAGGT
ACATCCGGCGAACAAGGCGTAGACACGGAAATTCCTGCCCGCAATAAAGAGTTAGCGGAGCGTGCAATTGCGGCC
GGTTTCGGTAAGTCTAGCTACTCTTCAATTATCGAAGTGCTGAAGAAATAA

>SeIRED
ATGAATAACGGCTTCGCTGCTCCTGTTACCGTCGTTGGACTCGGACCCATGGGGTGTGCGCTTGCAGATGCGTTT
CTCGCCGCTGGTCACCCGACTACAGTGTGGAATCGTTCGGCCCATAAGGCAGACCCGCTTGTGGCAAAGGGAGCC
GTTCGTGCGGCTACCGCTGCTGAAGCACTCGCCGCCAGCGACTTAGTGGTGGTTTGTGTCGCGGATTATGCTGCG
ATGCGTGCAGCCCTCGATCGCACCGGCGCAGAACTGAGTGGTAAAGTTCTCGTCAACCTCTGTTCCGGTACACCT
CGCGAGGCCCGCGAGGCTCTTACGTGGGCGACCGCGCACGGGGCTGGATATCTTGACGGTGCTATCATGGTGCCG
GTTGAAGTGATTGGTACCCCTAGTAGTGTTGTGTTTTATTCCGGTGCCCGTGAGCCATTTGACGCACACCGCTCA
ACGTTAGATGCCCTGGGTGGGGTGCCTCGCTACCTGGGAGATGACGCTGGGCTGGCAGTATTACACAATACCGCG
CTTTTGGGCTTGATGTGGGCTACGGTAAATGGGTTTCTTCACGCAGCCGCGCTCGTGGAAAGCGCGGGTGTCGGA
GTGGCTGACTTCGCCGAGACGGCAGTGGATTGGTTTCTGCCCTCGGTTATTGGCGAGATCTTACGTGCTGAGGCC
GCTCGCATTGACCGCGGTGAGTTCCCTGGCGATGGCGGGACCCTTGCGATGTGTTTAACAGCAATTGAACATATT
GTTCGTACCTCGCGCGATGCTGGAATCAGCGACGAGGTGCCGAGCCAGTTGAAGACATTGGGCGATCGTGCCGTA
GCGGCAGGTCACGGCGACGAGAACTACATGTCACTTATCAAGGTACTGCGCGTGCCTTCGACTGGTGCTCATCGT
TAA

Section S4. HPLC analysis

Table S4. HPLC chromatographic conditions and retention times for ketones and chiral amines. E_1 = enantiomer 1, E_2 = enantiomer 2.

Method A: *n*-hexane/isopropanol/diethylamine (97/03/0.1)
Method B: *n*-hexane/isopropanol/diethylamine (90/10/0.1)
Flow rate: 1 ml min^{-1}, monitored at wavelength of 265 nm

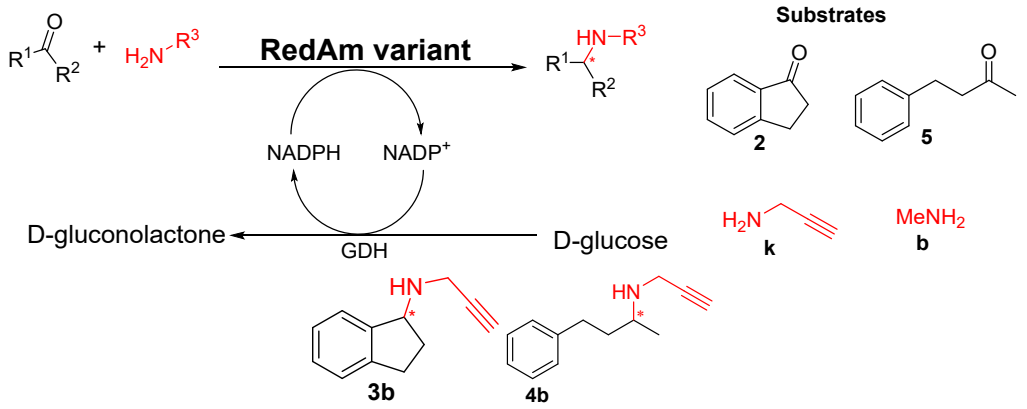

Ketone	Amine	Product	Column/Method	Relative response factor	Ketone retention time (min)	Product retention time (min)	
						E_1	E_2
3	**b**	**3b**	CHIRALPAK®NB-5 Method A	2.3	8.7	6.9 (*S*)	7.3 (*R*)
4	**b**	**4b**	CHIRALPAK®NB-5 Method A	1	7.7	6.9 (*R*)	7.2 (S)

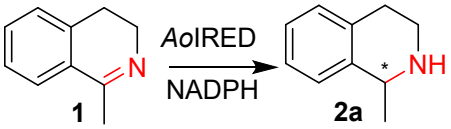

Imine	Amine	Column	Relative response factor	Imine retention time (min)	Product retention time (min)	
1	**2a**	CHIRALPAK®IC Method B	9.0		7.0 (*S*)	7.4 (*R*)

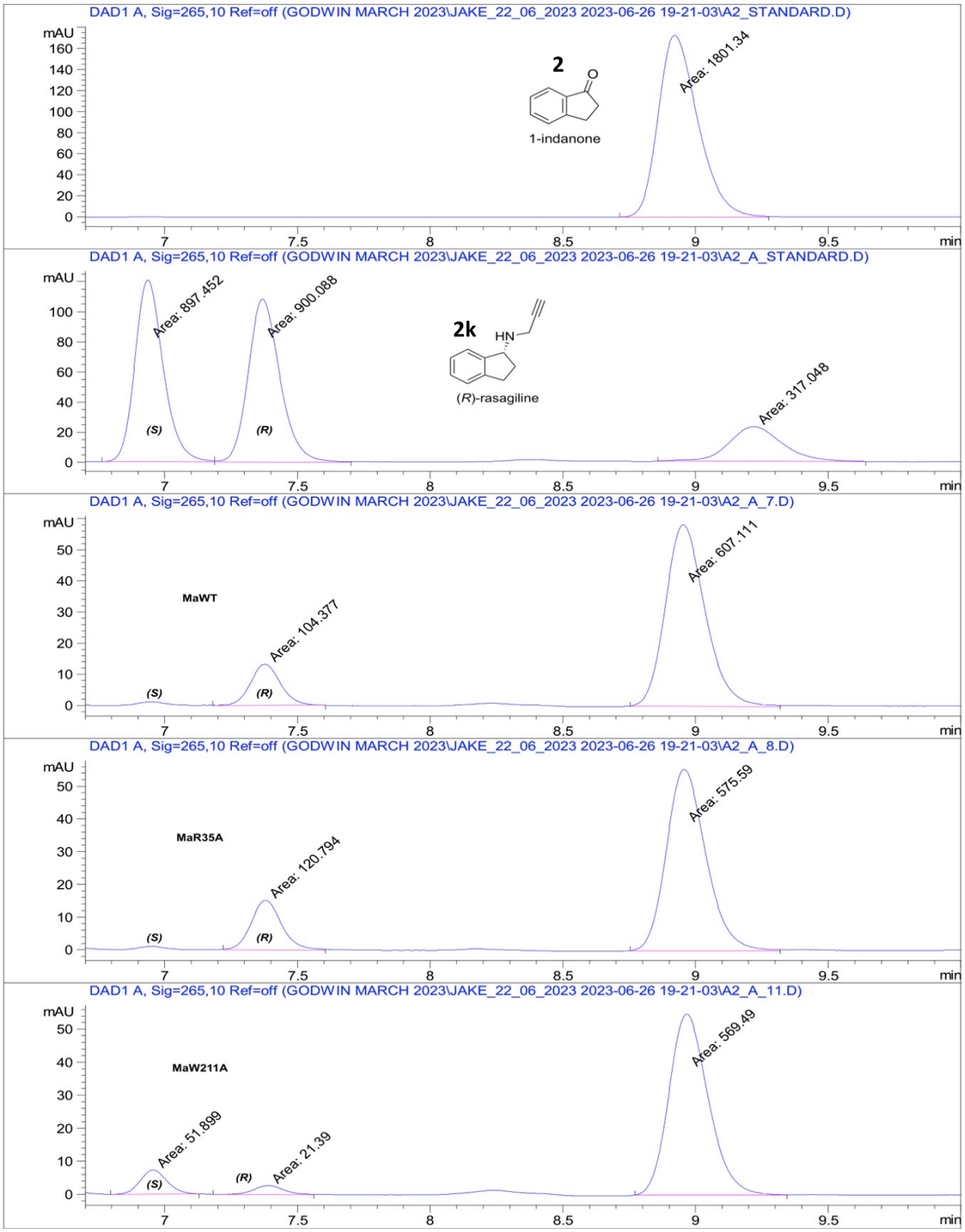

Figure S5. HPLC analysis of the *Ma*RedAm-catalysed reductive amination of ketone indanone **3** with propargylamine to form the chiral product **2k (3b in main manuscript)**. Top to bottom: ketone standard, product standard, and biotransformation data for purified MaRedAm WT and its R35A and W211A.

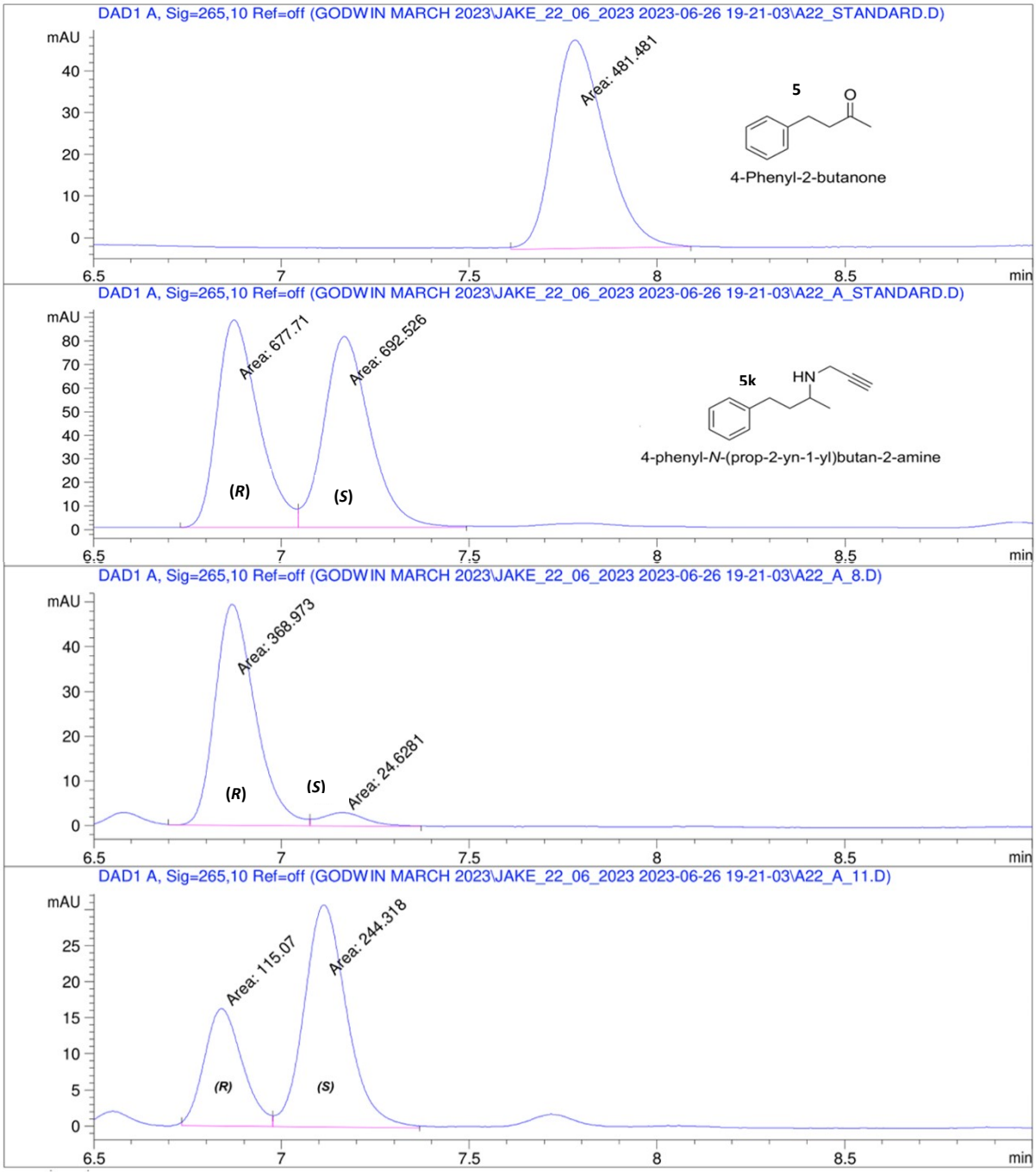

Figure S6. HPLC analysis of the *Ma*RedAm-catalysed reductive amination of 4-phenyl-2-butanone **4** with propargylamine to form the chiral product **2k** (**4b** in the main manuscript). Top to bottom: ketone standard, product standard, and biotransformation data for purified *Ma*RedAm WT and its R35A and W211A.

References

1 E. DeMott, D. J. Dickinson and R. Doonan, *MicroPublication Biol.*, **2021**, 10.17912/micropub.biology.000499.

2 G. Kim, S. Lee, E. Levy Karin, H. Kim, Y. Moriwaki, S. Ovchinnikov, M. Steinegger and M. Mirdita, *Nat. Protoc.*, 2024, 1–23.

3 M. L. Hekkelman, I. de Vries, R. P. Joosten and A. Perrakis, *Nat. Methods*, 2023, **20**, 205–213.

4 E. Krieger, K. Joo, J. Lee, J. Lee, S. Raman, J. Thompson, M. Tyka, D. Baker and K. Karplus, *Proteins Struct. Funct. Bioinforma.*, 2009, **77**, 114–122.

5 D. A. Case, H. M. Aktulga, K. Belfon, I. Ben-Shalom, S. R. Brozell, D. S. Cerutti, T. E. C. III, V. W. D. Cruzeiro, T. A. Darden, R. E. Duke, G. Giambasu, M. K. Gilson, H. Gohlke, A. W. Goetz, R. Harris, S. Izadi, S. A. Izmailov, C. Jin, K. Kasavajhala, M. C. Kaymak, E. King, A. Kovalenko, T. Kurtzman, T. Lee, S. LeGrand, P. Li, C. Lin, J. Liu, T. Luchko, R. Luo, M. Machado, V. Man, M. Manathunga, K. M. Merz, Y. Miao, O. Mikhailovskii, G. Monard, H. Nguyen, K. A. O'Hearn, A. Onufriev, F. Pan, S. Pantano, R. Qi, A. Rahnamoun, D. R. Roe, A. Roitberg, C. Sagui, S. Schott-Verdugo, J. Shen, C. L. Simmerling, N. R. Skrynnikov, J. Smith, J. Swails, R. C. Walker, J. Wang, H. Wei, R. M. Wolf, X. Wu, Y. Xue, D. M. York, S. Zhao and P. A. Kollman, *Amber 2021*, University of California, San Francisco, 2021.

6 C. I. Bayly, P. Cieplak, W. Cornell and P. A. Kollman, *J. Phys. Chem.*, 1993, **97**, 10269–10280.

7 J. Wang, R. M. Wolf, J. W. Caldwell, P. A. Kollman and D. A. Case, *J. Comput. Chem.*, 2004, **25**, 1157–1174.

8 G. A. Aleku, S. P. France, H. Man, J. Mangas-Sanchez, S. L. Montgomery, M. Sharma, F. Leipold, S. Hussain, G. Grogan and N. J. Turner, *Nat. Chem.*, 2017, **9**, 961–969.

9 C. Orlando, M. Prejanò, N. Russo and T. Marino, *ChemBioChem*, 2023, **24**, e202300412.

10 F. De Castro, G. Ciardullo, F. P. Fanizzi, M. Prejanò, M. Benedetti and T. Marino, *Int. J. Mol. Sci.*, 2023, **24**, 9849.

11 G. Ciardullo, A. Parise, M. Prejanò and T. Marino, *J. Chem. Inf. Model.*, 2024, **64**, 1593–1604.

12 J. A. Maier, C. Martinez, K. Kasavajhala, L. Wickstrom, K. E. Hauser and C. Simmerling, *J. Chem. Theory Comput.*, 2015, **11**, 3696–3713.